

Study of nano-particle deposition in tubular pipes under turbulent condition

Pouyan Talebizadeh^{1, a *}, Hassan Rahimzadeh^{1, b}, Goodarz Ahmadi^{2, c}, Kiao Inthavong^{3, d}, Meisam Babaie^{4, e}, Ali Zare^{5, f}, Thuy Van Chu^{5, g} and Richard Brown^{5, h}

¹Department of Mechanical Engineering, Amirkabir University of Technology, Iran

²Department of Mechanical and Aeronautical Engineering, Clarkson University, Potsdam, NY 13699, USA.

³School of Aerospace, Mechanical and Manufacturing Engineering, RMIT University, Australia.

⁴Petroleum and Gas Engineering Division, School of Computing, Science and Engineering (CSE), University of Salford, Manchester, United Kingdom.

⁵Biofuel Engine Research Facility, Queensland University of Technology, Australia.

^atalebizadeh.pouyan@gmail.com, ^brahimzad@aut.ac.ir, ^cgahmadi@clarkson.edu,

^dkiao.inthavong@rmit.edu.au, ^em.babaie@salford.ac.uk, ^fali.zare@qut.edu.au,

^gthuy.chuvan@hdr.qut.edu.au, ^hrichard.brown@qut.edu.au

Keywords: Nano-particle, Turbulent flows, Tubular pipes, Reynold stress transport model, Deposition velocity.

Abstract. This paper aims to study the deposition and dispersion of nano-particles in turbulent tubular pipe flows. In this work, the Eulerian-Lagrangian particle tracking method is used to simulate the transport of nano-particles in turbulent flows under the conditions of one-way coupling. In order to simulate the turbulent flow in a pipe, the Reynolds stress transport model (RSTM) is used with the help of CFD method. RSTM is one of the most accurate Reynolds-averaged Navier-Stokes methods. In addition, near wall region, Two-layer zonal model is employed in the CFD model to simulate the viscous sublayer separated from the fully-turbulent layer in the pipe. The results show that RSTM with Two-layer zonal model can well predict the turbulent flow and particle deposition velocity in tubular pipes. The output of this study can provide a guideline for evaluating the nano-particle transport and deposition in turbulent pipe flows.

Introduction

Dispersion and deposition of particles in turbulent pipe flows have received considerable attention due to its importance in a number of industrial and engineering applications [1]. Particle deposition in turbulent flows have been studied for many years. Wood [2] presented a simple semi-analytical expression for estimating particle deposition in both smooth and rough turbulent duct flows. The deposition velocity is defined as the ratio of the particle mass flux to the wall per unit area, relative to the ambient particle concentration. Li and Ahmadi [3] studied the deposition of small particles and considered the effects of Brownian motion, gravity and turbulence fluctuations for different Reynolds numbers. Fan and Ahmadi [4] presented a sublayer model for predicting particle deposition in vertical turbulent smooth and rough ducts. They also developed a semi-empirical equation for evaluating the deposition velocity on smooth and rough walls. Ounis et al. [5] did the first direct numerical simulation (DNS) of Brownian diffusion in a turbulent channel flow. Tian and Ahmadi [6] studied the nano- and micro-particle deposition in turbulent duct flows and considered the effects of Brownian, Saffman lift, gravity forces, and turbulence fluctuations. They found that the RSTM that accounts for the anisotropic behavior of turbulence provided more accurate description of the near wall flow. Furthermore, the use of the two-layer zonal boundary condition led to more accurate predictions compared with the standard wall function.

In this paper, the depositions of nano-particles in turbulent pipe flows were investigated using the Lagrangian particle tracking method. For this purpose, RSTM with two-layer zonal model as the wall functions was employed. The turbulent flow parameters including the mean velocity, RMS velocities, and dissipation rate, as well as, the particle deposition rates were evaluated and the results were compared with the available experimental and numerical data.

Mathematical modeling

Flow field simulation

For an incompressible fluid, the continuity and momentum equations for the mean motion in a turbulent flow are given as:

$$\frac{\partial \bar{u}_i}{\partial x_i} = 0 \quad (1)$$

$$\bar{u}_j \frac{\partial \bar{u}_i}{\partial x_j} = -\frac{1}{\rho} \frac{\partial \bar{p}}{\partial x_i} + \nu \frac{\partial^2 \bar{u}_i}{\partial x_j \partial x_j} - \frac{\partial}{\partial x_j} R_{ij} \quad (2)$$

where x_i is the position, \bar{u}_i is the mean velocity, \bar{p} is the mean pressure, ρ is the constant mass density, ν is the kinematic viscosity, and $R_{ij} = \overline{u'_i u'_j}$ is the Reynolds stress tensor. The fluctuation velocity component u'_i is defined as $u_i - \bar{u}_i$ where u_i is the instantaneous velocity. The RSTM which evaluates the components of turbulence stresses is given as:

$$\begin{aligned} \underbrace{\bar{u}_k \frac{\partial}{\partial x_k} R_{ij}}_{C_{ij}=\text{convection}} &= \underbrace{\frac{\partial}{\partial x_k} \left(\left(\frac{\nu_t}{\sigma^k} + \nu \right) \frac{\partial}{\partial x_k} R_{ij} \right)}_{D_{ij}=\text{diffusion}} - \underbrace{\left(\overline{u'_i u'_k} \frac{\partial \bar{u}_j}{\partial x_k} + \overline{u'_j u'_k} \frac{\partial \bar{u}_i}{\partial x_k} \right)}_{P_{ij}=\text{production}} \\ &- \underbrace{C_1 \frac{\varepsilon}{k} \left(R_{ij} - \frac{2}{3} \delta_{ij} k \right)}_{\phi_{ij,1}} - \underbrace{C_2 \left[(P_{ij} - C_{ij}) - \frac{1}{3} (P_{kk} - C_{kk}) \right]}_{\phi_{ij,2}} + \underbrace{\phi_{ij,w} - \frac{2}{3} \delta_{ij} \varepsilon}_{\varepsilon_{ij}=\text{dissipation}} \end{aligned} \quad (3)$$

$\phi_{ij} = \text{pressure strain}$

$\phi_{ij,w}$ (the wall reflection term) and all the other parameters are given in [7]. k is the fluctuation kinetic energy, ε is the turbulence dissipation rate and ν_t is the turbulent viscosity which are given as:

$$k = \frac{1}{2} \overline{u'_i u'_i} \quad (5)$$

$$\frac{\partial \varepsilon}{\partial t} + \bar{u}_j \frac{\partial \varepsilon}{\partial x_j} = \frac{\partial}{\partial x_j} \left[\left(\nu + \frac{\nu_t}{\sigma^\varepsilon} \right) \frac{\partial \varepsilon}{\partial x_j} \right] - C^{\varepsilon 1} \frac{\varepsilon}{k} R_{ij} \frac{\partial \bar{u}_i}{\partial x_j} - C^{\varepsilon 2} \frac{\varepsilon^2}{k} \quad (6)$$

$$\nu_t = C_\mu \frac{k^2}{\varepsilon} \quad (7)$$

In this study, the two-layer zonal model was employed for resolving the near-wall flow features [8]. This approach used a one-equation model to account the near-wall effect [9]. Here, k is calculated through its transport equation, while ε and ν_t are given as:

$$\varepsilon = k^{3/2} / l_\varepsilon \quad (8)$$

$$\nu_t = C_\mu \sqrt{k} l_\mu \quad (9)$$

The length scale l_ε and l_μ are given in [7]. Beyond the buffer layer, the default RSTM features were used [6]. To simulate turbulence fluctuations and its effects on particle dispersion in a turbulent flow field, the DRW model was used [10]. In this model, the fluctuation velocity is evaluated as:

$$u'_i = G \sqrt{u_i'^2} \quad (10)$$

where G is a zero mean, unit variance normally distributed random number and $\sqrt{u_i'^2}$ is the root mean-square (RMS) of the local turbulence fluctuation velocity in the i th direction which are determined directly from the RSTM. In the present approach, the particles interact with an eddy during the eddy

life time or the particle eddy crossing time. The effect of turbulence is then introduced with the use of the instantaneous fluid velocity ($u_i = \bar{u}_i + u'_i$) in the particle equation of motion.

Particle transport simulation

The nano-particle equation of motion including the Brownian force for particles is given as:

$$\frac{du_i^p}{dt} = \frac{18\mu}{d_p^2 \rho_p C_c} (u_i^g - u_i^p) + F_{Brownian} \quad (11)$$

where u_i^p and u_i^g are, respectively, the components of the particle and local fluid velocities, μ is the fluid viscosity. C_c is the Cunningham correction factor to the Stokes drag law and is given as:

$$C_c = 1 + \frac{2\lambda}{d_p} (1.257 + 0.4e^{-1.1d_p/2\lambda}) \quad (12)$$

where λ is the mean free path of air. The amplitude of the Brownian force is given as [5]:

$$F_{Brownian} = \zeta \sqrt{\frac{\pi S_0}{\Delta t}} \quad (13)$$

where ζ is a zero-mean, unit-variance independent Gaussian random number, Δt is the time-step for particle integration and S_0 is the spectral intensity function defined as:

$$S_0 = \frac{216\nu k_B T}{\pi^2 \rho_g d_p^5 S^2 C_c} \quad (14)$$

In the above equation, T is the fluid absolute temperature, k_B is the Boltzmann constant, S is the particle-to-fluid density ratio and ρ_g is the fluid density. In this study, motions of nanoparticles ranging from 5 to 200 nm, with a particle-to-fluid density ratio of $S=2000$ were simulated. Due to range of particle sizes, only the effects of Brownian diffusion and turbulent fluctuations were considered, and the effect of gravity on the nanoparticle deposition, which is negligibly small was neglect. In many cases, particle deposition rate is presented with use of the deposition velocity. For a uniform concentration C_0 near a surface, the deposition velocity is:

$$u_d = \frac{J}{C_0} \quad (15)$$

where J is the particle flux to the surface per unit areas per unit time. In Lagrangian particle tracking, for a uniform initial injection of N_0 particles distributed in a region within a distance of 30 wall units (H_0) from the wall, the deposition velocity is given as:

$$u_d = \frac{N_d / t_d}{N_0 / H_0} \quad (16)$$

where N_d is the number of deposited particles in the time duration t_d . Note that the wall unit is defined as ν / u^* . In practice, the time duration should be long enough to obtain a quasi-equilibrium condition where the rate of the total number of deposited particles reaches a constant value [11]. The non-dimensional form of the deposition velocity is give as u_d / u^* where u^* is the shear velocity defined as $\sqrt{\tau_w / \rho}$ and τ_w is the wall shear stress.

Results and Discussion

In this study, the mesh consisting entirely of hexahedral control volume are generated in ICEM CFD 15.0 with higher mesh resolution near the wall boundaries. Fig. 1 displays the schematic discretization of the computational domain at the cross section of the tube. The mesh includes 2,013,165 cells. Note that the diameter of the pipe is considered 4.5mm.

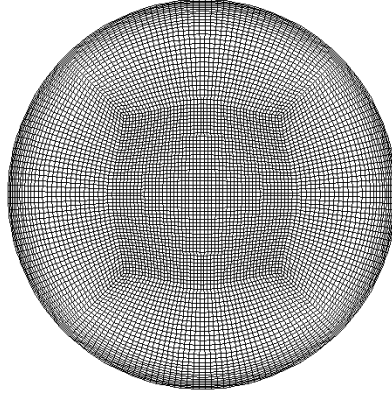


Fig. 1. The schematic discretization of the computational domain at the pipe cross section.

In this study, the mean velocity was 20 m/s, and the Reynolds number based on the pipe diameter was 6159. An inlet turbulence intensity of 2% was also assumed. The pipe length is sufficiently long so that the flow reaches to a fully developed turbulent flow and the corresponding particle deposition velocity. Under these conditions, the wall shear stress obtained from the FLUENT code was equal to 2.5 N/m² resulting in a shear velocity of 1.429 m/s. Figs. 2-a to 2-c display the mean velocity and turbulence profiles at three cross sections along the pipe beginning, middle and the pipe end. For all parameters, the data from the three locations collapse into one single line which indicated a fully developed turbulent region throughout the pipe.

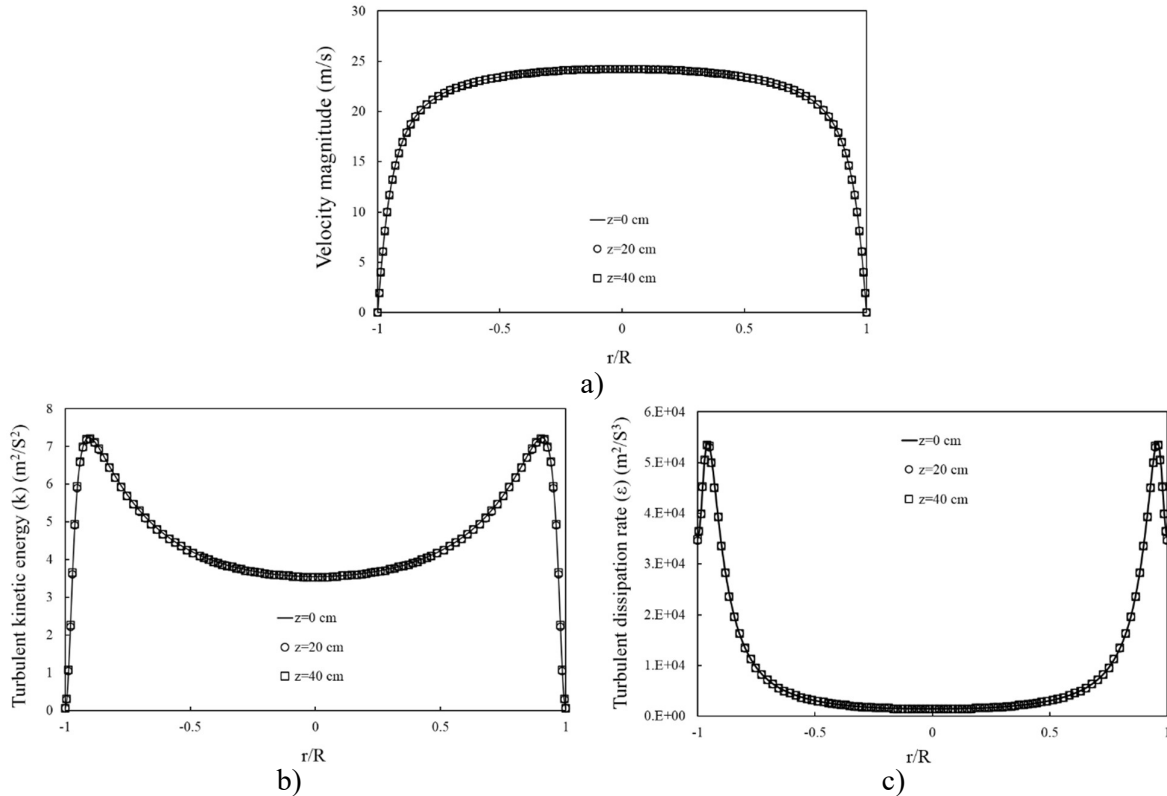


Fig. 2. Comparison of a) mean axial velocity, b) turbulence kinetic energy, and c) turbulence dissipation rate profiles at three pipe cross sections.

Fig. 3 compares the predicted non-dimensional stream-wise mean velocity profile in the wall region in compare with the semi-empirical equations for the viscous sublayer and the “log law” regions which are given in [6]. It is seen that the present results are in good agreement with the semi-

empirical results which provides confidence in the FLUENT code to simulate the near-wall turbulence mean velocity features in pipe flows.

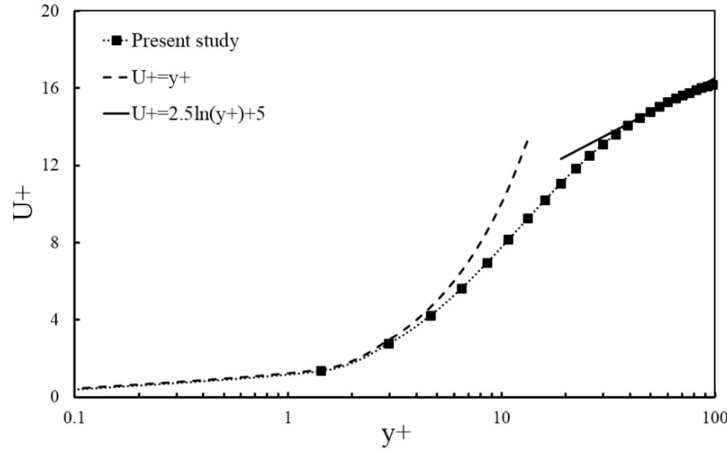


Fig. 3. Non-dimensional stream-wise mean velocity profile in wall units

Fig. 4 shows the predicted non-dimensional root mean square turbulence velocity fluctuations for the tubular pipe flow in compare with the DNS results of Kim et al. [12]. The velocity fluctuations are highly anisotropic in the near-wall region but approach isotropy toward the central region [6]. Furthermore, the present results are in acceptable agreement with the DNS results of Kim et al. [12].

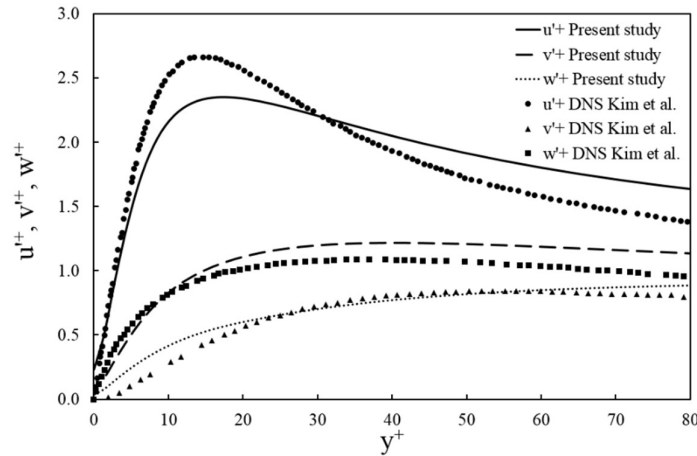


Fig. 4. Non-dimensional root mean square turbulence velocity fluctuations

For calculating the deposition velocity, $N_0=31836$ particles for the size range of 5 to 200 nm were simulated. The particles are initially injected from the area between two circles with the radius of R (2.25 mm) and $R-H_0$ and then the deposition efficiency is calculated by Eq. (16). Note that when a particle hits the wall, it will be deposited on the wall and then removed from the calculations. Fig. 5 compares the predicted deposition velocities with the empirical equations of Wood [2] and also Fan and Ahmadi [4]. It is seen the present model predictions are in good agreement with the empirical models. The results display the left leg of the V-shaped variation of the deposition velocity where it decreases to a minimum as particle diameter increases about 300 nm to 500 nm using the empirical correlations. The favorable comparison in Fig. 5 suggests that the Reynolds stress turbulent model with two-layer zonal wall function is capable of predicting turbulent flow features and nano-particle deposition in pipes. Note that the total number of deposited particles should reach to an equilibrium condition which corresponds to the constant particle deposition velocity.

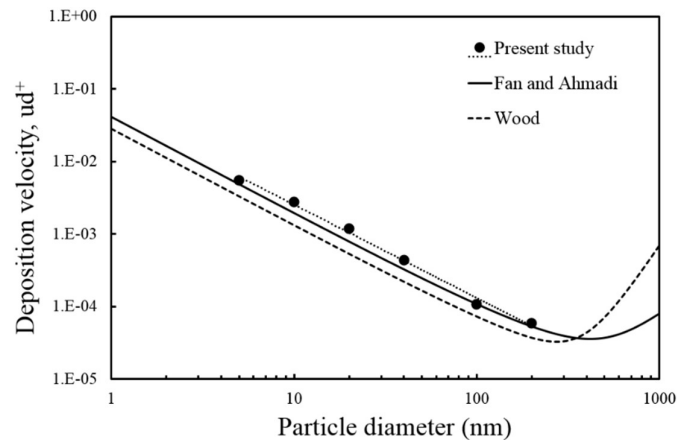


Fig. 5. Comparison of the predicted deposition velocity in a pipe with the empirical correlation.

Conclusions

In this paper, the nano-particle transport and deposition in turbulent pipe flows were investigated. The RSTM in conjunction with the two-layer zonal model was used to simulate the turbulent flow field. The corresponding instantaneous velocity fluctuations were generated using the eddy life time model. The Lagrangian particle tracking model was used to determine the particle trajectories under the assumption of one-way coupling. The simulation results show that the predicted deposition velocities for pipe are in good agreement with the earlier empirical equations. The study provided guidelines for evaluating nano-particle transport and deposition in turbulent pipe flows.

References

- [1] V. Golkarfard, P. Talebizadeh, Numerical Comparison of Airborne Particles Deposition and Dispersion in Radiator and Floor Heating Systems, *Advanced Powder Technology*, 25 (2014) 389-397.
- [2] N.B. Wood, A simple method for the calculation of turbulent deposition to smooth and rough surfaces, *Journal of Aerosol Science*, 12 (1981) 275-290.
- [3] A. Li, G. Ahmadi, Computer simulation of deposition of aerosols in a turbulent channel flow with rough wall, *Aerosol Science Technology*, 18 (1993) 11-24.
- [4] F. G. Fan, G. Ahmadi, A sublayer model for turbulent deposition of particles in vertical ducts with smooth and rough surfaces, *Journal of Aerosol Science*, 24 (1993) 45-64.
- [5] H. Ounis, G. Ahmadi, J.B. McLaughlin, Brownian particles deposition in a directly simulated turbulent channel flow, *Physics of Fluids A*, 5 (1993) 1427-1432.
- [6] L. Tian, G. Ahmadi, Particle Deposition in Turbulent Duct Flows - Comparisons of Different Model Predictions, *Journal of Aerosol Science*, 38 (2007) 377-397.
- [7] Ansys help viewer, in, 2013.
- [8] H.C. Chen, V.C. Patel, Near-wall turbulence models for complex flows including separation, *AIAA Journal*, 26 (1988) 641-648.
- [9] M. Wolfshtein, The velocity and temperature distribution in one-dimensional flow with turbulence augmentation and pressure gradient, *International Journal of Heat and Mass Transfer*, 12 (1969) 301-318.
- [10] P. Hutchinson, G.F. Hewitt, A.E. Dukler, Deposition of liquid or solid dispersions from turbulent gas streams: a stochastic model, *Chem. Eng. Sci.*, 26 (1971) 419-439.
- [11] C. He, G. Ahmadi, Particle deposition in a nearly developed turbulent duct flow with electrophoresis, *Journal of Aerosol Science*, 30 (1999) 739-758.
- [12] J. Kim, P. Moin, R. Moser, Turbulence statistics in fully developed channel flow at low Reynolds number, *Journal of Fluid Mechanics*, 177 (1987) 133-166.